



Characterization of residual stresses in Eurofer welded specimens: measurements by neutron diffraction and comparison with weld modeling

Roberto Coppola, Olivier Asserin, Philippe Aubert, Chedly Braham, Arnaud Monnier, Monica Valli, Eberhard Diegele

► To cite this version:

Roberto Coppola, Olivier Asserin, Philippe Aubert, Chedly Braham, Arnaud Monnier, et al.. Characterization of residual stresses in Eurofer welded specimens: measurements by neutron diffraction and comparison with weld modeling. Journal of Nuclear Materials, 2011, 417 (1-3), pp.51-54. 10.1016/j.jnucmat.2010.12.051 . cea-02284969

HAL Id: cea-02284969

<https://cea.hal.science/cea-02284969>

Submitted on 11 Dec 2023

HAL is a multi-disciplinary open access archive for the deposit and dissemination of scientific research documents, whether they are published or not. The documents may come from teaching and research institutions in France or abroad, or from public or private research centers.

L'archive ouverte pluridisciplinaire **HAL**, est destinée au dépôt et à la diffusion de documents scientifiques de niveau recherche, publiés ou non, émanant des établissements d'enseignement et de recherche français ou étrangers, des laboratoires publics ou privés.



Characterization of residual stresses in Eurofer welded specimens: Measurements by neutron diffraction and comparison with weld modeling

R. Coppola^{a,*}, O. Asserin^b, P. Aubert^b, C. Braham^c, A. Monnier^b, M. Valli^d, E. Diegele^e

^a ENEA-Casaccia, UTTFISSM, Via Anguillarese 301, 00123 Roma, Italy

^b CEA, DEN, DM2S, SEMT, LTA, F-91191, Gif-sur-Yvette, France

^c ENSAM, 151 Blvd de l'Hôpital, 75013 Paris, France

^d ENEA-Faenza, UTMATF, Via Ravennana 186, 48018 Faenza, Italy

^e Fusion for Energy (F4E) C/Josep Pla 2 – Ed. B3, 7a planta, 08019 Barcelona, Spain

ARTICLE INFO

Article history:

Available online 24 December 2010

ABSTRACT

The stress field of a dual-beam laser weld on a Eurofer-97 model plate has been experimentally determined by neutron diffraction measurements. The measurements were carried out at the ILL-Grenoble, in the three principal directions, at different distances from the weld and inside the weld itself. In the longitudinal direction, the most relevant for technical applications, there is good agreement between these experimental results and results obtained by finite element numerical methods: tensile stresses as high as 750 MPa are found inside the weld, rapidly decreasing with increasing distance from the weld centre. In the two other directions the agreement between experimentally determined and calculated stresses is still good far from the weld; inside the weld the experimental data are affected by the strong texture detected by X-ray diffraction, possibly produced by the heating and subsequent cooling of the structure.

© 2010 Elsevier B.V. All rights reserved.

1. Introduction and material characterization

Assembly of test blanket modules (TBM) manufactured from EUROFER-97 needs several different welding and joining techniques, where laser welding processes are among the most promising. Advantages of laser processes include that less distortion and a narrower fusion zone are procured due to the higher cooling rate. This process could be used for the stiffening grid assembly, which requires a lot of welds in a very complex structure. The present work has been carried out in the frame of the development of high quality Eurofer welds for Helium Cooled Lithium–Lead test blanket modules (TBM) relevant to develop the DEMO blanket. Neutron diffraction measurements have been made on a prototype mock-up to provide an experimental determination of the residual stresses produced by the welding and compare them with the calculated values. This will contribute in assessing the reliability of such welded structures in view of their planned use in a tokamak. Additional X-ray diffraction measurements have been made to complement the neutron measurements of the weld. The assembly evaluated is a laser welded EUROFER-97 plate with integral cooling channels; it is $90 \times 100 \times 8$ mm in size with the weld running along the plate centre (Fig. 1). The welding was conducted by two YAG laser of peak power 4 kW, at a velocity of 5.8 mm s^{-1} . The numerical simulation of the process, carried out by CEA using

Finite Element Analysis (FEA), included thermo-metallurgical modeling and residual stress simulation [1,2]. The analyses take into account that phase transformations, involving both austenitic and ferritic–martensitic phases, occur in the EUROFER steel during thermal treatments. The heat source was modelled by the Cylindrical Involution Normal formula, widely used in a variety of welding processes, and by two symmetrical peripheral conic heat sources, which determined the shape of the molten pool. This lead to simulated thermo-metallurgical results in good agreement with the experimental ones, namely concerning the characteristics of the molten pool and the micro-hardness behaviour [2].

2. Experimental technique and data analysis

Reference is made to [3–5] for a general discussion of the use of neutron diffraction for strain and stress determination. The measurement of strains by neutron or X-ray diffraction is based on the well known Bragg law $2d_{hkl} \sin \theta = \lambda$ relating the crystallographic lattice spacing characterized by Miller indices hkl , d_{hkl} , with the wavelength, λ and the angle θ where the reflection is observed. Defining the strain ε as

$$\varepsilon = \frac{(d - d_0)}{d_0} \quad (1)$$

where d and d_0 are strained and reference lattice parameters respectively. The strain ε can be determined by the shift in the maximum of the Bragg peaks; the broadening of these peaks is

* Corresponding author. Tel.: +39 0630484724; fax: +39 0630484747.

E-mail address: roberto.coppola@enea.it (R. Coppola).

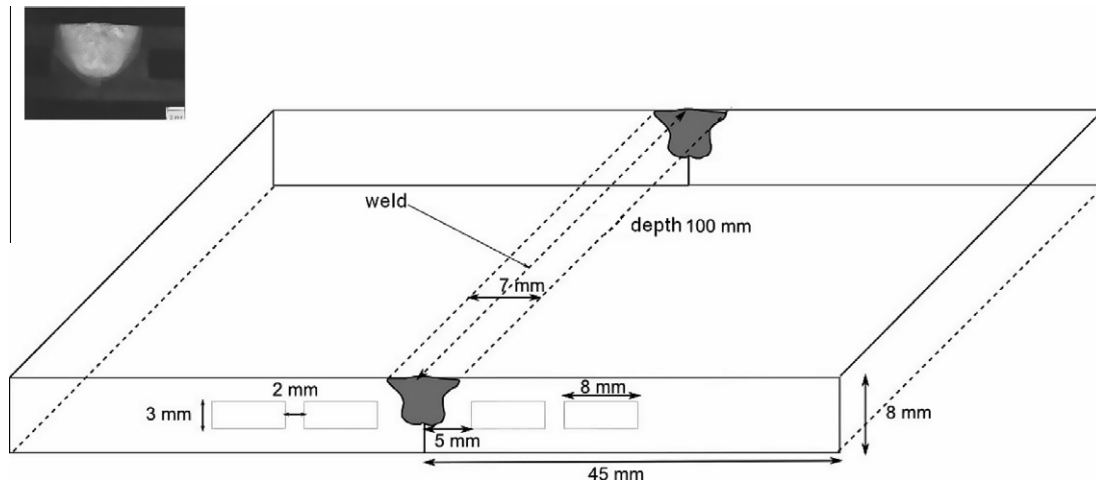


Fig. 1. Scheme of the investigated EUROFER welded plate and a cross-sectional picture of the weld (after [2]). The principal stress axes are the longitudinal direction (along the weld, in the plane of the plate), the transverse direction (the direction across the weld line, in the plane of the plate) and the normal direction (normal to the surface of the plate). The neutron diffraction measurements were carried out at mid-length of the plate, at different distances from the weld centre.

characterized by their full width at half maximum (FWHM), related to crystallographic grain size or local variations of strains. The three principal components of the stress tensor σ are obtained from the equation

$$\sigma = E\varepsilon \quad (2)$$

where E is the Young modulus of the investigated material. The main advantage of using neutron beams compared to X-rays is their deeper penetration of the materials, reaching a few mm in certain cases.

The neutron diffraction measurements were carried out, at room temperature, at the “SALSA” strain diffractometer [6] installed at the High Flux Reactor of the Institute Max von Laue–Paul Langevin (ILL), in Grenoble. The neutron wavelength was 0.169407 nm and the selected crystallographic reflection (2 1 1). Three mutually perpendicular directions with respect to the sample were defined (Fig. 2): longitudinal (along the length of the weld path, in the plane of the plate), transverse (across the weld line, in the plane of the plate), normal (normal to the surface of the plate). The slits defining the incident and the diffracted neutron beam gave a diffracting volume of $1 \times 1 \times 2.5 \text{ mm}^3$ (2.5 mm high) in the transverse and normal directions and of $1 \times 1 \times 0.5 \text{ mm}^3$ (0.9 mm high) in the longitudinal direction. The measurements were taken at 0, 5, 10, 20 and 40 mm from the weld centreline on one side of the weld at a depth of 1.25 mm from the top surface

and at mid-length of the plate. Residual strains (ε) were calculated using the equation

$$\varepsilon = \frac{\Delta\theta}{\tan\theta} \quad (3)$$

where $\Delta\theta$ is the difference between the measured angle and strain-free Bragg angle (θ_0). The ‘strain-free’ diffraction angle ($2\theta_0$), providing d_0 , was chosen as the average of the values measured at the position 40 mm from the weld centre (far-field average). Assuming X, Y, Z as the principal directions of deformation, then the stresses obtained are the principal stresses. The longitudinal (σ_x), transverse (σ_y) and normal (σ_z) direction residual stresses are given by

$$\begin{aligned} \sigma_x &= \frac{E}{(1+\nu)(1-2\nu)} [(1-\nu)\varepsilon_x + \nu(\varepsilon_y + \varepsilon_z)] \\ \sigma_y &= \frac{E}{(1+\nu)(1-2\nu)} [(1-\nu)\varepsilon_y + \nu(\varepsilon_x + \varepsilon_z)] \\ \sigma_z &= \frac{E}{(1+\nu)(1-2\nu)} [(1-\nu)\varepsilon_z + \nu(\varepsilon_x + \varepsilon_y)]. \end{aligned} \quad (4)$$

Residual stresses were calculated [7] from the three perpendicular strains using Eq. (4), where it was assumed $E = 217 \text{ GPa}$ and the Poisson ratio $\nu = 0.33$, that is the same values used in the FEA calculations [2].

3. Results

Fig. 3 shows the strain values obtained for the three components, while Fig. 4 shows the corresponding FWHM values. The obtained stresses in longitudinal, transverse and normal directions are shown in Figs. 5–7 respectively; and for comparison, the corresponding calculated stress values are included in each figure. In the longitudinal direction (Fig. 5), the neutron diffraction data give stress values raising up to approximately 750 MPa in the centre of the weld, in good agreement with the calculated values; increasing the distance from the weld the experimental stresses decrease to $\sim 50 \text{ MPa}$, a value slightly higher on average than the calculated value. In the transverse direction (Fig. 6) good agreement with the calculated stresses is found far from the weld, while inside the weld the neutron data consistently measure higher stresses than the calculated values. Also in the normal direction there is good agreement between experimental and calculated data far from the weld, but inside the weld experimental values as high as 700 MPa are found.

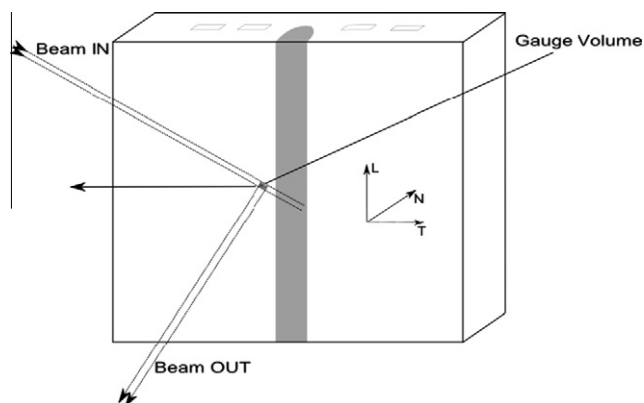


Fig. 2. Sample and weld orientation with respect to the neutron beam in the three investigated directions.

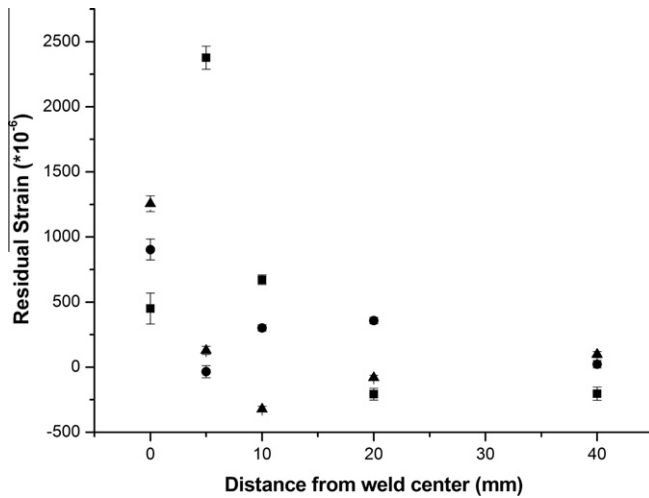


Fig. 3. Longitudinal (squares), transverse (dots) and normal (triangles) strains as a function of the distance, in mm, from the weld centre.

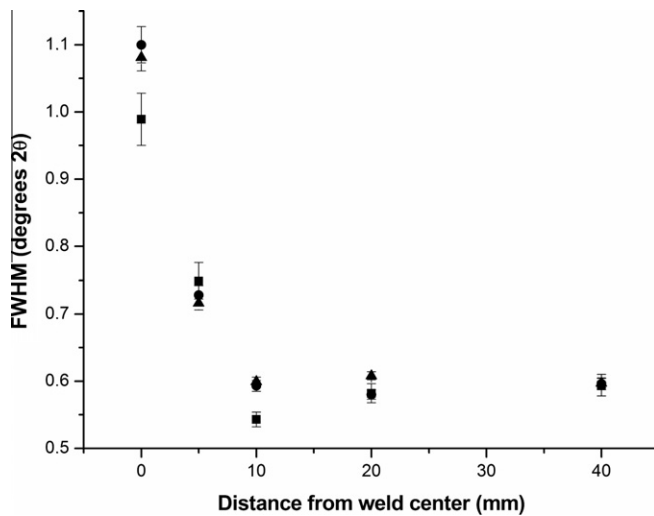


Fig. 4. Longitudinal (squares), transverse (dots) and normal (triangles) FWHM values as a function of the distance, in mm, from the weld centre.

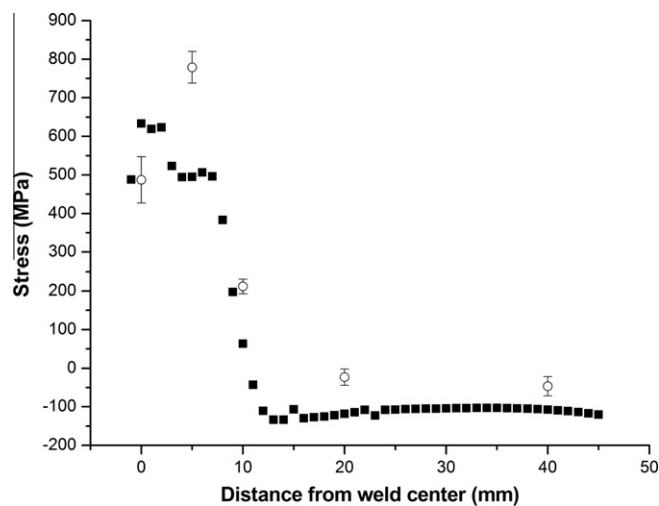


Fig. 5. Longitudinal stresses in MPa (dots) determined by neutron diffraction as a function of the distance, in mm, from the weld centre ('0'). For comparison, the longitudinal and calculated stresses are shown, indicated by squares [2].

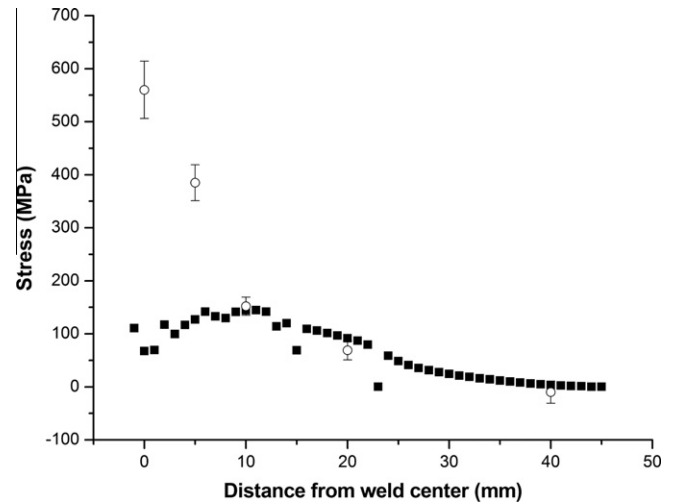


Fig. 6. Transverse stresses in MPa (dots) determined by neutron diffraction as a function of the distance, in mm, from the weld centre ('0'). For comparison, the transverse calculated stresses are shown, indicated by squares [2].

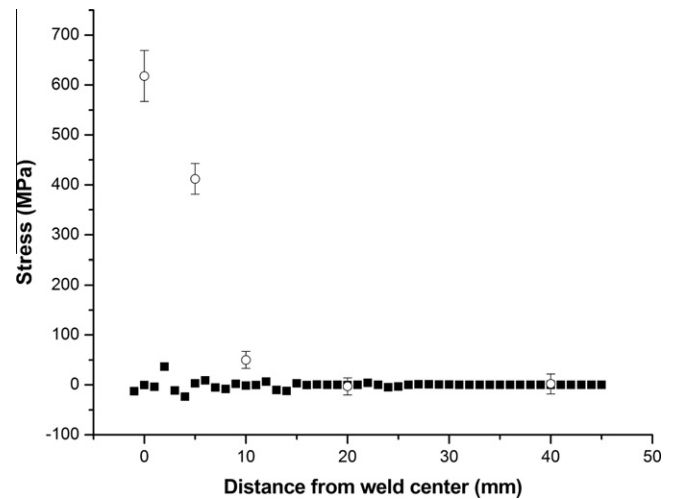


Fig. 7. Normal stresses in MPa (dots) determined by neutron diffraction as a function of the distance, in mm, from the weld centre ('0'). For comparison, the normal calculated stresses are shown, indicated by squares [2].

The microstructure inside the Heat Affected Zone (HAZ) has been investigated by X-ray diffraction in order to assess the 'strain-free' lattice variation between the base material and the weld. A strong crystallographic texture is detected in the weld leading to difficult interpretation of the X-ray measurements. It is also noted that for both techniques, neutron (Fig. 4) and X-ray, the FWHM increases approaching the weld, which suggests a high density of microstrains in the weld and in the HAZ in agreement with the simulated micro-hardness results [1]; similar results were found in similar welds of ferritic/martensitic steels for fusion applications [8]. In fact, complex metallurgical transformations, including re-austenisation and $M_{23}C_6$ carbide precipitation, occur in the weld and in the HAZ, which are expected to have inhomogeneous distributions after the welding process. That is reflected in strong gradients in the strain field in this region, with a large uncertainty on the d_0 value and, consequently, on the experimentally determined strains and stresses. Based on these experimental data, the FEA calculations are shown to predict quite reliably the stress field in the longitudinal direction, which is the most relevant for technical applications. Further refinements will be necessary to

fully understand the stress fields in the weld centre, both by experimental data and by numerical simulations. Far from the HAZ the agreement between experimental neutron data and numerical simulation is quite satisfactory in all three directions.

4. Conclusions

The stress field has been experimentally determined by neutron diffraction measurements in a dual-beam laser weld on an EURO-FER-97 model plate with integrated cooling channels. The measurements were carried out in the three principal directions, at different distances from the weld and inside the weld itself. In the longitudinal direction, which is the most relevant for technical applications, good agreement is found between the experimental results and those obtained by FEA numerical methods: tensile stresses as high as 750 MPa are found inside the weld, rapidly decreasing with increasing the distance from the weld centre. In the other two directions the agreement between experimentally determined and calculated stresses is still good far from the weld, but inside the weld the experimental data are probably affected by the strong texture produced by the heating and subsequent cooling during the high-temperature welding process. Further refinements are therefore necessary, both in experimental data and in numerical simulations, to fully understand the stress distribution inside this weld.

Acknowledgements

This work, supported by the European Commission under the contract of Associations, was carried out within the framework of the European Fusion Development Agreement. The views and opinions expressed herein do not necessarily reflect those of the European Commission. Dr. D. Hughes (ILL) is acknowledged for valuable collaboration in the experiment and related data analysis.

References

- [1] O. Asserin, Rapport Technique DTH/2006/94 (2006) (available upon request to the author).
- [2] A. Monnier, O. Asserin, Rapport Technique DM2S SEMT/LTA/RT/08-004/A (2008) (available upon request to the authors).
- [3] M.T. Hutchings, C.G. Windsor, in: K. Sköld, D.L. Price (Eds.), *Methods of Experimental Physics, Neutron Scattering*, vol. 23, Academic, 1987, p. 405.
- [4] G. Windsor, in: M. Fontana, F. Rustichelli, R. Coppola (Eds.), *Industrial and Technological Applications of Neutrons*, North Holland, 1992, pp. 167–200.
- [5] R. Coppola, C. Nardi, in: M.E. Fitzpatrick, A. Lodini (Eds.), *Analysis of Residual Stress by Diffraction using Neutron and Synchrotron Radiation*, Taylor & Francis, 2003, pp. 319–333.
- [6] D. Hughes, T. Pirling, G. Bruno, P.J. Whithers, *Mater. Sci. Eng. A* 437 (2006) 139.
- [7] ISO/TTA 3:2001(E), *Polycrystalline Materials – determination of residual stresses by neutron diffraction*, International Organization for Standardization, CP 56, CH-211 Geneva 20, Switzerland, 2001.
- [8] C. Braham, M. Ceretti, R. Coppola, A. Lodini, C. Nardi, in: *Proceeding ICRS5 Conference*, Linköping, June 1997, pp. 169.